Journal of Macromolecular Science, Part A
Publication details, including instructions for authors and subscription information:
http://www.informaworld.com/smpp/title~content=t713597274

Synthesis and Properties of Poly(4,8-dialkoxy-1,5-naphthalenevinylene)s

Hung-Te Chang[a]; Hsun-Tsing Lee[b]
[a] Department of Chemical Engineering, Wufeng Institute of Technology, Chia Yi, Taiwan, ROC [b] Department of Chemical and Materials Engineering, Vanung University, Chung Li, Taiwan, ROC

To cite this Article Chang, Hung-Te and Lee, Hsun-Tsing(2009) 'Synthesis and Properties of Poly(4,8-dialkoxy-1,5-naphthalenevinylene)s', Journal of Macromolecular Science, Part A, 46: 7, 722 — 726
To link to this Article: DOI: 10.1080/10601320902939556
URL: http://dx.doi.org/10.1080/10601320902939556

Journal of Macromolecular Science®, Part A: Pure and Applied Chemistry (2009) **46**, 722–726
Copyright © Taylor & Francis Group, LLC
ISSN: 1060-1325 print / 1520-5738 online
DOI: 10.1080/10601320902939556

Synthesis and Properties of Poly(4,8-dialkoxy-1,5-naphthalenevinylene)s

HUNG-TE CHANG[1,*] and HSUN-TSING LEE[2]

[1] *Department of Chemical Engineering, Wufeng Institute of Technology, Chia Yi, Taiwan, ROC*
[2] *Department of Chemical and Materials Engineering, Vanung University, Chung Li, Taiwan, ROC*

Received July 2008, Accepted January 2009

Novel conjugated materials, poly(4,8-dialkoxy-1,5-naphthalenevinylene)s (OC_n-PNV, n = 4, 6, 8, and 12), have been prepared by a method similar to the Gilch procedure. The structure, optical and thermal properties of these polymers with various alkoxy side chain lengths have been evaluated by IR, UV-Vis absorption, fluorescence emission and thermogravimetric analysis. The band gap of OC_n-PNV increases with increasing side chain length. Moreover, wavelengths of the photoluminescence (PL) emission peaks (λ_{max}) of OC_n-PNV solutions decrease with increasing alkoxy side chain length. This is probably due to the entanglement of long side chains that causes distortion of the conjugated main chains and thereby raises band gap of the polymer. PL λ_{max}'s of these polymers in film state are red-shifted by 14–59 nm than those in solution state. The red-shift is due to the more chain aggregations after spin coating from solution into film state and consequently the lower band gap in the film state. Besides, the polymer with shorter side chains is more thermally stable than that with longer side chains.

Keywords: conjugated materials, poly(4,8-dialkoxy-1,5-naphthalenevinylene)s, thermal properties, photoluminescence

1 Introduction

After the discovery of polyacetylene as a new class of conjugated polymers by Shirakawa *et al.* (1), a great deal of research has focused on the development of other conjugated polymers. Conjugated polymers derive the unusual semi-conducting properties from having a framework of alternating single and double carbon-carbon bonds. Conjugated polymers may be prepared by either chemical or electrochemical methods (2–4). In recent years, there has been considerable progress made with the polymerization of conjugated aromatic polymers such as polyfluorene (5), polyaniline (6), polythiophene (7), and polypyrrole (8). The unusual optoelectronic properties of these aromatic polymers have developed them for potential applications in various optoelectronic devices such as photovoltaic cells (9), transistors (10), and light-emitting diodes (11). This has promoted the synthesis of soluble conjugated polymers with various substituted side-chains. For example, poly(*p*-phenylenevinylene) derivatives are soluble luminescent materials for use in light-emitting diodes (LEDs) (12–14).

Different conjugated polymers exhibit their own electro-optical properties (15). Even the tetrathiafulvalene (TTF) dimer with divinylnaphthalene spacer possesses charge transfer property (16). In this work, we synthesized and characterized the novel conjugated poly(4,8-dialkoxy-1,5-naphthalenevinylene)s (OCn-PNVs) with various lengths of alkoxy side chain via a series of organic chemical reactions and the Gilch polymerization method (17). Furthermore, the effects of side chain length on the polymers' optical and thermal properties are studied.

2 Experimental

2.1 Materials

1,5-dihydroxynaphthalene, 1-bromobutane, 1-bromohexane, 1-bromooctane, 1-bromo dodecane, paraformaldehyde, hydrobromic acid (31 wt% in acetic acid), potassium hydroxide (KOH), tetrabutylammonium bromide (TBAB) and acetic acid were purchased from Fluka Chemical (Ronkonkoma, NY). Potassium *tert*-butoxide (*t*-BuOK) was purchased from Sigma-Aldrich (Steinheim, Germany). All the above reagents were synthetic grade and used as received. Tetrahydrofuran (THF) was synthetic grade and purchased from Tokyo Chemical Industry Co. (Tokyo, Japan), which was dried over sodium and distilled prior to use.

---

[*] Address correspondence to: Hung-Te Chang, Department of Chemical Engineering, Wufeng Institute of Technology, Chia Yi, Taiwan, ROC. Tel.: +886-5-226 7125 ext. 22354; Fax: +886-5-206 3264; E-mail: cht421@ yahoo.com.tw

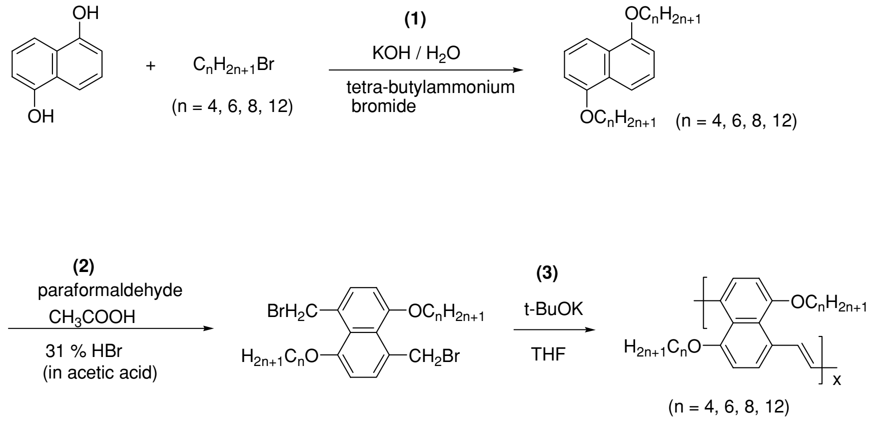

Sch. 1. Synthesis route for the monomers and polymers.

2.2 Instruments

NMR spectra were measured by the Bruker Avance DPX-400 spectrometer (400 MHz). FT-IR spectra were recorded by the Perkin-Elmer Model Spectrum One spectrometer. UV-Vis absorption spectra were measured by the Shimadzu Model UV-160 spectrophotometer with a specimen concentration of about 0.11 wt%. Fluorescence spectra were recorded by the Aminco-Bowman Model Thermo Spectronic Series 2 spectrophotometer with a specimen concentration of about 0.11 wt%. Average molecular weights of polymers were measured by a gel permeation chromatographer (GPC) of the Analytical Scientific Instrument Model 500 system. Polystyrene standards were used for molecular weight calibration and tetrahydrofuran was used as carrier solvent. Thermal gravimetric analyses were performed on the Perkin-Elmer Model TGA-7 thermogravimetric analyzer (TGA) with a heating rate of 10°C/min and under a nitrogen stream. Prior to the thermal analysis, each specimen was subject to a heating scan from room temperature to 100°C in the TGA furnace to remove any adsorbed moisture.

2.3 Synthesis Process

The synthesis route for the monomers and polymers is illustrated in Scheme 1. The monomers were prepared via chemical reactions as alkylation (1) and bisbromomethylation (2) from the starting material 1,5-dihydroxynaphthalene. Finally, the conjugated polymer, OCn-PNVs (n = 4, 6, 8, 12) were obtained by a method similar to the Gilch procedure (3).

2.3.1. *Alkylation of 1,5-dihydroxynaphthalene*

The 1,5-dibutoxynaphthalene (DOC$_4$-N), one representative of 1,5-dialkoxy naphthalene (DOC$_n$-N, n = 4, 6, 8, 12), was obtained by the following typical procedure. A solution mixture of 1,5-dihydroxynaphthalene (4.77 g, 29 mmol), potassium hydroxide (4.18 g, 75 mmol), 25 mL H_2O, and tetra-butyl ammonium bromide (5.73 g, 178 mmol) was stirred for 15 min. Then butyl bromide (10.33 g, 75 mmol) was added into the solution mixture. The reaction proceeded with stirring and heating at 80°C for 22 h. After the completion of the reaction, the solution was cooled to room temperature. The precipitated product was filtered, washed with H_2O (2×50 ml) and dried under dynamic vacuum. ^{1}H-NMR and ^{13}C-NMR spectra were used to confirm the formation of 1,5-dibutoxynaphthalene. The resonance peaks of ^{1}H-NMR (400 MHz, $CDCl_3$, δ ppm) spectrum are: 7.86 (d, J = 8.4 Hz, 2H); 7.35 (t, J = 8.0 Hz, 2H); 6.82 (d, J = 7.64 Hz, 2H); 4.13 (t, J = 6.32 Hz, 4H); 1.91 (m, J = 7.0 Hz, 4H); 1.60 (m, J = 7.48 Hz, 4H); 1.03 (t, J = 7.4 Hz, 6H). The resonance peaks of ^{13}C NMR (400 MHz, $CDCl_3$, δ ppm) spectrum are: 154.7 (C_1, C_5); 126.8 (C_9, C_{10}); 125.0 (C_3, C_7); 114.0 (C_4, C_8); 105.2 (C_2, C_6); 67.8 ($OCH_2CH_2CH_2CH_3$); 31.4 ($OCH_2CH_2CH_2CH_3$); 19.5 ($OCH_2CH_2CH_2CH_3$); 13.9 ($OCH_2CH_2CH_2CH_3$).

Similarly, the other three 1,5-dialkoxynaphthalenes, designated as DOC$_6$-N, DOC$_8$-N and DOC$_{12}$-N, were obtained from the reactions between 1,5-dihydroxynaphthalene and alkyl bromides with alkyl chain lengths of 6, 8 and 12 carbons, respectively. The appearance and yields of all 1,5-dialkoxynaphthalene are shown in Table 1. ^{1}H-NMR and ^{13}C-NMR spectra of the DOC$_6$-N, DOC$_8$-N and DOC$_{12}$-N are similar to those of the DOC$_4$-N except the more complicated methylene (CH_2) group signals.

Table 1. The appearance and yields of 1,5-dialkoxynaphthalene

Monomer	*Appearance*	*Yield (%)*
DOC$_4$-N	Dark brown solid	90
DOC$_6$-N	Dark brown solid	95
DOC$_8$-N	Dark brown solid	90
DOC$_{12}$-N	Dark brown solid	95

2.3.2. *Bis-bromomethylation of 1,5-dialkoxy-naphthalene*

1,5-dibutoxy-4,8-bisbromomethylnaphthalene (BBMDOC_4-N) was obtained by the following typical procedure. A 6 mL solution of HBr in acetic acid (31 wt%) was added to the suspension of 1,5-dibutoxynaphthalene (15.1 mmol) and paraformaldehyde (0.93 g, 31 mmol) in glacial acetic acid (50 mL). The mixture was stirred and heated at 50°C for 24 h. After cooling to room temperature, the reaction solution was poured into 300 mL ice-cold water. The dark green precipitates were filtered, washed with H_2O (2 × 50 mL) and dried under dynamic vacuum. ^{1}H-NMR and ^{13}C-NMR spectra were used to confirm the formation of BBMDOC_4-N. The resonance peaks of ^{1}H-NMR (400 MHz, $CDCl_3$, δ ppm) spectrum are: 7.34 (d, J = 8.2 Hz, 2H); 6.83 (d, J = 8.16 Hz, 2H); 5.30 (s, 6H); 4.12 (t, J = 6.76 Hz, 4H); 2.02 (m, J = 7.16 Hz, 4H); 1.57 (m, J = 7.56 Hz, 4H); 1.01 (t, J = 7.44 Hz, 6H). The resonance peaks of ^{13}C-NMR (400 MHz, $CDCl_3$, δ ppm) spectrum are: 157.1 (C_1, C_5); 131.3 (C_4, C_8); 126.5 (C_9, C_{10}); 125.7 (C_3, C_7); 106.9 (C_2, C_6); 68.8 ($OCH_2CH_2CH_2CH_3$); 39.0 (CH_2Br); 31.0 ($OCH_2CH_2CH_2CH_3$); 19.6 ($OCH_2CH_2CH_2CH_3$); 13.8 ($OCH_2CH_2CH_2CH_3$).

Likewise, the other three 1,5-dialkoxy-4,8-bisbromomethylnaphthalenes, designated as BBMDOC_6-N, BBMDOC_8-N and BBMDOC_{12}-N,were obtained from the reactions among paraformaldehyde, HBr and 1,5-dialkoxynaphthalenes with alkoxy chain lengths of 6, 8 and 12 carbons, respectively. The appearance and yields of all 1,5-dialkoxy-4,8-bisbromomethylnaphthalenes are shown in Table 2. ^{1}H-NMR and ^{13}C-NMR spectra of the BBMDOC_6-N, BBMDOC_8-N and BBMDOC_{12}-N are similar to those of the BBMDOC_4-N except the more complicated methylene (CH_2) group signals.

2.3.3. *Polymerization*

Table 3. The average molecular weights and yields of OC_n-PNVs (n = 4, 6, 8, 12)

Polymer	$^{(a)}M_n$	$^{(b)}M_w$	$^{(c)}Dp$	$^{(d)}$ *Yield (%)*
OC_4-PNV	5472	31655	19	25–34
OC_6-PNV	6679	26469	19	19–20
OC_8-PNV	8067	23724	20	17–25
OC_{12}-PNV	5302	20131	10	17–20

A 4.3 mL solution of potassium *tert*-butoxide in THF (0.3 M) was slowly syringed into the solution of 4,8-bisbromomethyl-1,5-dialkoxynaphthalene (1.2 mmol) in THF (4.3 mL) with stirring, under N_2 atmosphere and at room temperature over 10 min. Then another 11.8 mL solution of potassium *tert*-butoxide in THF (0.3 M) was syringed into the solution with stirring, under N_2 atmosphere and at room temperature for 24 h. After the completion of reaction, the resultant viscous solution was diluted with 50 mL THF. The precipitates were obtained by adding 130 mL methyl alcohol with stirring overnight. The brown precipitates were filtered, washed with methyl alcohol (2 × 50 mL) and dried under dynamic vacuum. The average molecular weights and yields of OC_n-PNVs (n = 4, 6, 8, 12) are shown in Table 3.

Table 2. The appearance and yields of 1,5-dialkoxy-4,8-bisbromomethylnaphthalene

Monomer	*Appearance*	*Yield (%)*
BBMDOC_4-N	Dark green solid	78
BBMDOC_6-N	Dark green solid	86
BBMDOC_8-N	Dark green solid	89
BBMDOC_{12}-N	Dark green solid	91

(a) Mn: number average molecular weight.
(b) Mw: weight average molecular weight.
(c) Dp: degree of polymerization.

3 Results and Discussion

3.1 Structure Analysis of OC_n-PNV

Figure 1 shows FT-IR spectra of the OC_n-PNV (n = 4, 6, 8, 12). Comparing these spectra, the peak wavenumbers are invariant with side chain length. However, many peaks are broadened with a higher n value. This indicates that the structure is more non-uniform for a polymer with longer side chain. Thus, the stretching or vibration of a functional group occurs in a broader wavenumber range (18). The peak at 3086 cm^{-1} is due to the C-H stretching of aromatic ring (19). The peaks at 2984 and 2889 cm^{-1} are due to C-H stretching of the alkyl side chains and those at 1606 and 1525 cm^{-1} are due to the C=C stretching of aromatic ring (19). The peaks at 1457 and 1388 cm^{-1} are due to the –CH_2- segmental bending of alkyl side chains and the one at 1273 cm^{-1} is due to the asymmetric C-O-C bond stretching (13). The peak at 1198 cm^{-1} is due to the C-H in plane bending of aromatic ring and the one at 1062 cm^{-1} is due to

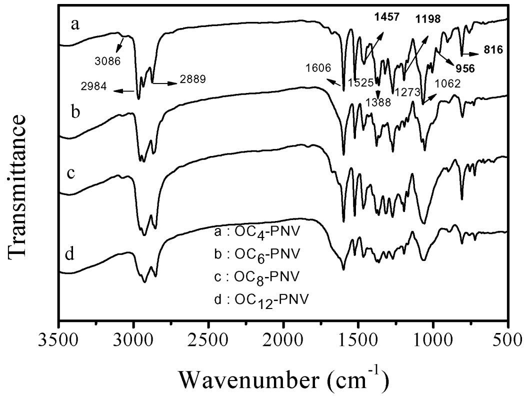

Fig. 1. FT-IR spectra of OCn-PNV (n = 4, 6, 8, 12).

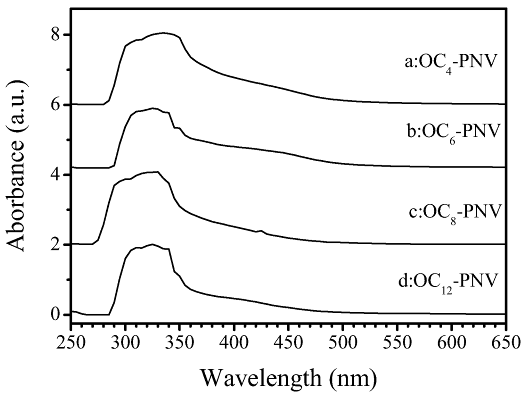

Fig. 2. UV-Vis absorption spectra of the OCn-PNV (n = 4, 6, 8, 12) in THF (0.11 wt%).

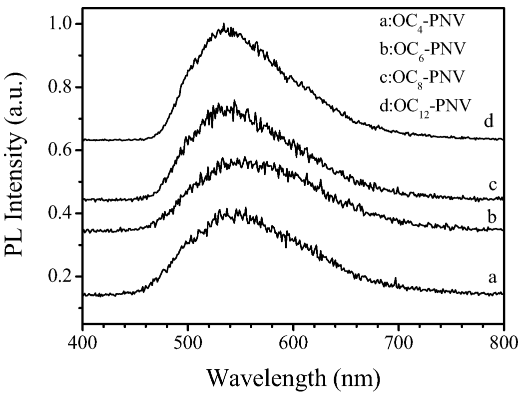

Fig. 3. Photoluminescence spectra of the OCn-PNV (n = 4, 6, 8, 12) in THF (0.11 wt%) with an excitation wavelength of 320 nm.

the symmetric C-O-C bond stretching (13). Moreover, the peak at 956 cm^{-1} is due to the C-H out-of-plane bending of trans-vinylene unit (19) and the one at 816 cm^{-1} is due to the C-H out-of-plane bending of aromatic ring. The results of FT-IR spectra confirm the formation of OC$_n$-PNV.

3.2 Optical Properties of OC$_n$-PNV

Figure 2 shows UV-Vis absorption spectra of the OC$_n$-PNV (n = 4, 6, 8, 12) in THF with a concentration of 0.11 wt%. The absorption peaks for all the OC$_n$-PNVs are broad and appear mainly in the range of 285–370 nm. These peaks are associated with the $\pi - \pi^*$ transition of conjugated naphthalenevinylene segments. On the other hand, the absorption edges are 531, 522, 506 and 498 nm, respectively for OCn-PNV with n = 4, 6, 8 and 12. The optical or band gap energy (E, in eV) is described by the following Equations 1 and 2:

$$\mathrm{E} = \frac{hc}{\lambda} \tag{1}$$

$$1\,\mathrm{eV} = 1.602 \times 10^{-19}\,\mathrm{Joule} \tag{2}$$

Where h is the Planck constant (6.63×10^{-34} Joule-s), c is the light velocity (3×10^8 m/s), and λ is the wavelength of absorption threshold. Using the value of absorption edge or threshold (λ) 531, 522, 506 and 498 nm, respectively, we deduce the band gaps for OCn-PNV (n = 4, 6, 8, 12) as 2.33, 2.37, 2.45 and 2.49 eV. The longer side chain length is, the higher band gap of OCn-PNV. The reason is that the easier entanglement of the longer side chains causes more distortion of the conjugated main chains and thereby raises the band gap of the polymer. Furthermore, the values of band gaps of these four polymers are higher than that of dialkoxy substituted PPV (2.1 eV) (20). This phenomenon indicates a distortion of the conjugated structure of OCn-PNV and an increase of the band gap.

Figure 3 shows photoluminescence (PL) emission spectra of the solutions (0.11 wt%) of OC$_4$-PNV, OC$_6$–PNV, OC$_8$-PNV and OC$_{12}$–PNV in THF with an excitation wavelength of 320 nm. The emission peaks ($\lambda_{\max}$) are at 555, 553, 543 and 534 nm for OC$_4$-PNV, OC$_6$–PNV, OC$_8$-PNV and OC$_{12}$–PNV, respectively. The polymer with longer side chains exhibits lower $\lambda_{\max}$ in its PL emission spectrum. This is probably due to the entanglement of long side chains that causes distortion of the conjugated main chains and thereby raises band gap energy of the polymer. The polymer with higher band gap energy would have lower $\lambda_{\max}$ in its PL emission spectrum. Therefore, the length of alkoxy side chains influences the conformation and conjugation length of the polymer.

Figure 4 shows PL emission spectra of the OC$_4$-PNV, OC$_6$–PNV, OC$_8$-PNV and OC$_{12}$–PNV films with an excitation wavelength of 320 nm. The emission peaks ($\lambda_{\max}$) are at 614, 567, 566 and 556 nm for OC$_4$-PNV, OC$_6$–PNV, OC$_8$-PNV and OC$_{12}$–PNV, respectively. The polymer with longer side chains in the film state also exhibits lower $\lambda_{\max}$ in its PL emission spectrum as the aforementioned result in solution state. Comparing Figure 3 with Figure 4, the emission peak (614 nm) of OC$_4$-PNV in film state shows a 59 nm red-shift relative to that (555 nm) in dilute solution state. The red-shift may be due to the changing of conjugated

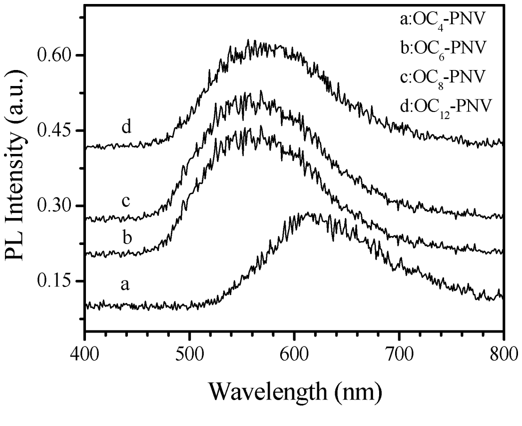

Fig. 4. Photoluminescence spectra of the OCn-PNV (n = 4, 6, 8, 12) films with an excitation wavelength of 320 nm.

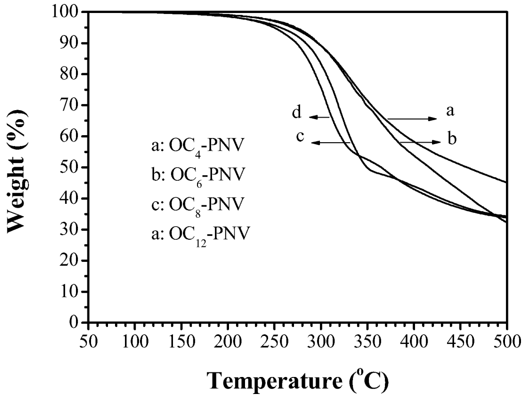

Fig. 5. TGA thermograms of OC$_n$–PNV (n = 4, 6, 8, 12).

main chains from the coiled conformation in solution state to extended conformation in aggregated solid state and thereby the lower band gap energy in film state. The other three polymers also exhibit the same solvatochromic effect. The red-shift of the PL emission peaks are 14, 23, and 22 nm for OC$_6$-PNV, OC$_8$-PNV and OC$_{12}$-PNV, respectively, when changing the polymer from solution to film state.

3.3 Thermal Stability of OC$_n$-PNV

Figure 5 shows TGA results of the OC$_n$-PNV (n = 4, 6, 8, 12). There are no appreciable weight losses below 200°C for these four polymers. The weight losses begin to increase pronouncedly at 250°C, at which the decomposition of alkoxy side chains starts to occur. The weight losses of OC$_4$-PNV, OC$_6$-PNV, OC$_8$-PNV, and OC$_{12}$-PNV are 10.8 wt%, 10.9 wt%, 16.7 wt%, and 24.2 wt%, respectively, as the temperature increases to 300°C. The weight loss above 400°C is due to the decomposition of the rigid and conjugated main chains as that of poly(p-phenylenevinylene) derivatives (21). The more pronounced weight loss of polymer with longer side chains than that with shorter side chains above 250°C is due to the easier decomposition of the alkoxy side chains than the rigid main chains. Thus, the polymer with shorter side chains is more thermally stable than that with longer side chains. OC$_4$-PNV is the most thermally stable compound among these four polymers.

4 Conclusions

Starting from 1,5-dihydroxynaphthalene, new poly(4,8-dialkoxy-1,5-naphthalenevinylene)s (OC$_n$-PNV, n = 4, 6, 8, and 12) had been successfully synthesized via sequential organic reactions as alkylation of 1,5-dihydroxynaphthalene, bis-bromomethylation of 1,5-dialkoxy-naphthalene and dehydrohalogenation of 1,5-dialkoxy-4,8-bisbromomethylnaphthalene. The $\pi - \pi^*$ transition energy of naphthalene vinylene segments in the polymer is invariant with the side chain length. Meanwhile, the band gaps of OC$_4$-PNV, OC$_6$–PNV, OC$_8$-PNV and OC$_{12}$–PNV are 2.33, 2.37, 2.45 and 2.49 eV, respectively. The PL λ_{max}'s of these four polymers in film state are red-shifted by 14 – 59 nm as compared to those in solution state. The red-shift is due to the less coiled conformation of the conjugated main chains and thereby the lower band gap in film state. Moreover, the polymer with shorter side chains is more thermally stable than that with longer side chains.

References

1. Chiang, C.K., Fincher, C.R., Park, Y.W., Heeger, A.J., Shirakawa, H., Louis, E.J., Gau, S.C., and MacDiarmid, A.G. (1977) *Phys. Rev. Lett.*, 39, 1098–1101.
2. Toba, M., Terashima, T., Nakashima, T., and Kawai, T. (2008) *Jpn. J. Appl. Phys.*, 47, 1371–1373.
3. Cecile, C., Mellah, M., Labbeö, E., Neödeö lec, J.Y., and Peörichon, J. (2002) *New J. Chem.*, 26, 787–790.
4. Yamamoto, T., and Hisashi Kokubo, H. (2005) *Electrochimica Acta*, 50, 1453–1460.
5. Chen, P., Yang, G.Z., Wang, C.M., Wang, W., Wang, M., and Liu, T. (2007) *Polym. Int.*, 56, 996–1005.
6. Jin, Z., Su, Y., and Duan, Y. (2001) *Synth. Met.*, 122, 237–242.
7. Li, X. and Li, Y., (2003) *J. Appl. Polym. Sci.*, 90, 940–946.
8. Ansari, R. (2006) *E-Journal of Chemistry*, 3, 186–201.
9. Kittichungchit, V., Shibata, T., Noda, H., Tanaka, H., Fujii, A., Oyabu, N., Abe, M., Morita, S., and Ozaki, M. (2008) *Jpn. J. Appl. Phys.*, 47, 1094–1097.
10. Krumm, J., Eckert, E., Glauert, W.H., Ullmann, A., Fix, W., and Clemens, W., (2004) *Electron Dev. Lett., IEEE*, 25, 399–401.
11. Sohn, S., Park, K., Lee, D., Jung, D., Kim, H.M., Manna, U., Yi, J., Boo, J.H., Chae, H., and Kim, H. (2006) *Jpn. J. Appl. Phys.*, 45, 733–3736.
12. Johansson, D.M., Srdanov, G., Yu, G., Theander, M., Inganas, O., and Andersson, M. (2000) *Macromolecules.*, 33(7), 2311–2314.
13. Chang, H.T., Lee, H.T., Chang, E.C., and Yeh, M.Y. (2007) *Polym. Eng. Sci.*, 47, 1380–1387.
14. Shin, D.C., Kim, Y.H., You, H., and Kwon, S.K. (2003) *Macromolecules*, 36, 3222–3227.
15. Leclerc, M. (2001) *J. Polym. Sci. Part A: Polym. Chem.*, 39, 2867–2873.
16. Gonaleöz, S., Martin, N., Segura, J.L., and Seoane, C. (1998) *Tetrahedron Lett.*, 39, 3051–3054.
17. Gilch, H.G., and Wheelwright, W.L. (1966) *J. Polym. Sci. Part A-1*, 4, 1337–1349.
18. Fawcett, A.H. Polymer Spectroscopy: Deformation Studies of Polymers using Raman Spectroscopy, Fawcett, A. H., Ed. Publication: John Wiley & Sons Ltd.: West Sussex, England, 217–218, 1996.
19. Bradley, D.D.C. (1987) *J. Phys. D:Appl. Phys.*, 20, 1389–1410.
20. Trad, H., Ltaief, A., Majdoub, M., Bouazizi, A. and , Davenas, J. (2006) *Mater. Sci. Eng.*, C26, 340–343.
21. Chang, H.T., Lee, H.T., and Yeh, M.Y. (2007) *J. Appl. Polym. Sci.*, 103, 2734–2741.